Random Modeling of Optimal Economic, Security and Environmental Operation of Micro-grid by Managing Responsive Loads and Charging and Discharging Electric Vehicles

Alireza Bakhshinejad[1], Abdolreza Tavakoli[2*], Maziar Mirhosseini Moghaddam[3]
1- Department of Engineering, Lahijan Branch, Islamic Azad University, Lahijan, Iran.
Email: alireza.bakhshinejad @gmail.com
2- Department of Engineering, Lahijan Branch, Islamic Azad University, Lahijan, Iran.
Email: tavakoli@liau.ac.ir (Corresponding author)
3- Department of Engineering, Lahijan Branch, Islamic Azad University, Lahijan, Iran.
Email: m.mirhosseini@liau.ac.ir

Received: August 2020 Revised: November 2020 Accepted: January 2021

ABSTRACT:
The micro-grid operator must provide the energy required by its customers at the lowest cost and consider issues such as greenhouse gas emissions and security. The operator is faced with a multi-objective optimization problem in which customer demand must be provided at the lowest cost and safely. This research provides a new energy management system for islanded micro-grids. The small size of the islanded micro-grids, the high level of intermittent operation and the low inertia of distributed generation of inverter energy production resources make the frequency and voltage security two vital factors in the energy management system, which must be managed alongside economic-environmental policies. In this study, two practical tools are provided to help with the optimal operation and increase the profitability of the micro-grid operator. The first tool is the optimal and managed use of the V2G mode of electric vehicles. In the proposed approach, not only the penetration of electric vehicles in the network is managed but also this equipment is used to solve some of the network's challenges. The second tool is responsive loads and demand response programs in order to achieve the goals of the micro-grid operator. Covering the uncertainty of renewable energy sources by responsive loads, and how to model a demand response program in a micro-grid, are followed in this study. The strategy pursued several goals, including reducing energy and load costs, reducing the cost of charging EVs, and improving network parameters and security, such as voltage and frequency. The results confirm the effectiveness of the proposed approach.

KEYWORDS: Optimal Operation, Stochastic Model, Demand Response, Voltage Safety, Frequency Safety, Electric Vehicles, Renewable Energy Resources.

1. INTRODUCTION

In recent years, the dramatic growth in electricity consumption and limited fossil energy resources has prompted operators of power systems in various countries to seek new ways for managing consumption and supply energy to customers. The results of some researches indicate that in the future years, the high cost of extracting fossil energy resources will not permit them to be operated [2]. On the other hand, the environmental pollution of these energy sources and the problems of global warming, and international treaties have limited their usage in recent years. These issues have increased the tendency of governments to invest in renewable and clean energy resources. The main problem of renewable energy plants is the high cost of investment to build them [3]. On the other hand, with the growth and development of the science of restructuring and the development of privatization in the electricity industry, the pattern of operating power networks has changed. In the past, the operation of power grids was centralized, meaning that the network operator, on behalf of all manufacturers and consumers, the optimal production plan was determined based on the minimum cost of energy supply required by the subscribers.

Paper type: Research paper
DOI: https://doi.org/10.52547/mjee.15.2.15
How to cite this paper: A. Bakhshinejad, A. Tavakoli and M. Mirhosseini Moghaddam, "**Random Modeling of Optimal Economic, Security and Environmental Operation of Micro-grid by Managing Responsive Loads and Charging and Discharging Electric Vehicles**", *Majlesi Journal of Electrical Engineering*, Vol. 15, No. 2, pp. 15-37, 2021.

Introducing the benefits of privatization, the development of measuring and control devices, the limitation of fossil energy resources, environmental pollution, the advancement of technology in the operation of renewable energy sources, etc. change the strategy of operating power systems, from centralized to decentralized and have led to the appearance of smart micro-grids [4].

One of the most important challenges for micro-grid users is to maintain system security. One of the reasons for the difficulty of maintaining micro-grid security is that the production of distributed generation power plants is based on renewable energy, which depends on uncertain resources such as wind speed and sunlight. Any error in predicting these uncertain sources will cause the balance of production and consumption to be lost and the frequency and voltage of the network to be disrupted. This challenge is even more important when the micro-grid is being used separately from the global network. Unlike synchronous generators, most distributed generation power plants require electronic power devices for connecting to the micro-grid. The low inertia of these devices reduces the loadability, complexity of the control system, and compromises the security of the system. Therefore, variations in subscriber consumption and uncertainty of sunlight and wind (and thus fluctuations in the production of solar and wind units) as well as low inertia of distributed generations can compromise the security of the frequency and voltage of the micro-grid. Failure to pay attention to frequency and voltage in the production planning of distributed generation units, besides endangering network security, may impose economic losses to the operation of the micro-grids[5].

So far, several articles have been published about the optimal operation of micro-grids and their challenges. In [6], the role of demand response in thermal-wind production programming is considered using probabilistic programming. In this reference, researchers have dealt with the modeling of responsive loads in two modes of response based on encouragement and accountability based on pricing and have provided models for them. The results of this study show that responsive loads have a significant effect on reducing operating costs. In [7], the programming of renewable products and demand response in a network is analyzed. The researchers first modeled responsive loads and renewable production resources, including wind and solar power, and defined the objective function. In this study, researchers are using probabilistic programming to solve the problem. The results of the research show that if the demand response programs are used, it is possible to cover the fluctuations of wind and solar power. In [8], a frequency-dependent operation model has been proposed for intelligent micro-grid energy management. In this reference, optimal energy planning and reservation are determined in such a way that both economic and security goals are achieved. In [9], primary and secondary frequency control loops have been considered in the production planning of a micro-grid, although the uncertainty of sources of production based on renewable energy and the requirements of micro-grid frequency security and demand response capacities (in improving micro-grid security) have been ignored. In [10], a new model for the operation of micro-grids in the electricity market environment is presented. The micro-grid includes a wind turbine, a micro-turbine, and a residential consumer, and a battery-powered energy storage system. There is also a parking lot in the micro-grid that can be fed to network-connected vehicle and the energy stored in the vehicles can be sometimes used. The mentioned micro-grid is managed cooperatively, so that the parking lot, wind turbine, microturbine, and battery are at the disposal of the micro-grid manager. In the proposed model, the micro-grid participates in both the buyer and the seller in the distribution network market and suggests using game theory in the market. In [11], a smart parking lot has been simulated and analyzed to charge grid-connected hybrid electric vehicles. In using these parking lots, the main approach is to control the process of charging the vehicles in order to take advantage of the economic and environmental benefits of these vehicles and prevent the occurrence of unwanted loads on the network. Smart parking software, by being aware of the network situation, including low load, intermediate and high load, as well as receiving the real-time signal of the price of electricity on the one hand and the customer charging parameters, on the other hand, allocates power to the vehicles charger. In [12], network charging of hybrid electric vehicles is planned, taking into account the high percentage of penetration of these vehicles in the network. The goal is to improve the load profile of the distribution network when the vehicle is charging. For the convenience of the customer, the charge is assumed to be charged at home. In [13], a new method has been proposed to quantify the effect of charging EVs that may be distributed on the network security level. Network security is monitored by analyzing the single event N-1 before and after charging EVs at home. In [14], the behavior of these vehicles is modeled using binary and normal distributions and it is tried to provide an almost complete probabilistic model that covers the required parameters such as energy limitation, charging programming, etc. and how to calculate the optimal power to participate in the ancillary services market is described. Also, using these probability distributions, the optimal amount of power to participate in the ancillary services market is obtained according to the penal mechanisms. In [15], a two-level optimization has been proposed for the operation of a hybrid micro-grid (24 hours) with load forecasting and renewable

production. In [16], consumers' responses to different pricing schemes on the network have been studied at the distribution level. This research was conducted in a smart network environment. In this case, consumers have full access to immediate consumption and pricing information. Each consumer has an automatic demand response system to control the load with the applied price variations. Electric vehicles have also been introduced as a mobile energy storage unit, and the following function is intended for them in the smart grid.

- Area peak load displacement
- Respond to frequency fluctuations
- Operation as an emergency power supply
- Stabilization of the power of distributed generations

In [17], Multi-objective utilization planning has been investigated in an intelligent micro-grid system with responsive loads. In this reference, researchers are looking for optimal operation of an intelligent distribution system in the presence of distributed generation sources such as diesel generators, fuel cells, wind turbines, and solar cells in the presence of responsive loads. The authors solve the problem in a multi-objective way by using responsive loads to try to cover the uncertainty from wind and solar sources. To improve the efficiency of this research, the following can be recommended:

- Modeling the types of participant loads in demand response programs
- Penetration management of electric vehicles
- Considering appropriate and practical solutions for implementing demand response programs
- Considering the costs of operation and pollution separately

In this research, a management plan for micro-grid operators with a multi-objective, economic, technical, and security approach, environmental, and reliability has been presented. The low inertia of Distributed Generation Resources (DGs) and the high penetration of Renewable Energy Sources (RESs) disrupt the safety and stability of micro-grids, especially in island mode. Based on the proposed model, planning of controllable units on the production side is done not only to maintain the stability and security of the frequency and voltage of the micro-grid but also for the economic purpose of maximizing the expected benefit of the Micro-Grid Operator (MGO) and the environmental goal of minimizing pollutant production. Due to the dependence of renewable energy production capacity on climatic conditions, in this model, a new solution has been proposed to operate the system under uncertainty.

The proposed plan also includes the management of the penetration of electric vehicles into the micro-grid structure. For proper integration of electric vehicles with the grid and their use as a production unit using network connection technologies (V2G), electric vehicles have penetrated the micro-grid surface. The penetration of electric vehicles, especially in smart distribution networks and micro-grids, has caused serious challenges for the operators of micro-grids, especially during peak hours. The proposed management plan in this study has turned these problems into opportunities by proper management and controlling the challenge. In other words, with the proposed management plan, the energy stored in electric vehicles is returned to the grid in order to be used. These resources in addition to covering uncertainty, with proper management namely charging during the hours when electricity prices are low and discharging during peak hours and rising electricity prices, increase the operator's benefit greatly. In addition to production units and charging and discharging stations for electric vehicles, the proposed model has also provided a good way to participate in more loads in order to achieve more benefits. The proposed model for responsive loads makes it possible to analyze the effect of customer participation in DR programs on the economy and security in island mode. In this model, customers who participate in the DR program are divided into three general categories: price-sensitive loads, voltage-sensitive loads, and frequency-sensitive loads. The load position in the proposed model is considered to have a more accurate result. The vast majority of studies have used DC load flow in the optimization model. This unrealistic approximation causes ignoring the reactive power of programming and its significant effect on node voltage and even system frequency (if the lines are resistive). However, in the proposed approach, using AC-OPF, the frequency and voltage deviation planning and decision-making are done to compensate for them. Besides, the effect of DR resource participation on voltage regulation and micro-grid frequency is also investigated.

2. THE STRUCTURE OF THE PROPOSED MODEL

In this research, distributed energy resources include Distributed Controllable Generations (DGs) and distributed resources based on Renewable Resources (RESs) as well as Responsive Loads (DR) and Electric Vehicles (EVs) have been managed to meet the goals of the system and eliminate technical and security constraints. In this process, the MGO (Micro-Grid Operator) plays a key role as a supervisor of the optimal planning process and decision monitoring. To participate in customers in the DR program and the management of V2G and G2V electric vehicles, consumers are assumed to be equipped with intelligent measuring equipment and a Building Energy Management System (BMS).

The environmental information required by the MGO is received through communication lines and other required information, such as the amount of RESs

production and the amount of demand, is generated through predication methods, which are described below. MGO solves a problem of security-constrained optimization with the goal of energy planning and management charge and discharge of electric vehicles and responsive loads on the planning horizon to find optimal solutions according to the goals of the system.

2.1. Solution Method

The input data in the proposed structure consists of two categories: Deterministic data and stochastic data which are obtained by modeling random processes. This is done in order to model the uncertainty in the production of wind (WT), solar (PV) resources and the demand of customers, with the aim of minimizing the amount of forecast error. Accordingly, several scenarios are initially generated based on Probability Density Functions (PDF). Then, using a scenario reduction algorithm, the N_s- scenario is selected to model the uncertainty. In the next step, the reduced scenarios are used in the process of optimization modeling based on Mixed-Integer Linear Programming (MILP), in order to maximize the expected benefit of MGO by considering voltage and frequency security and DR and V2G management.

2.2. Modeling the Uncertainty of Production of Renewable Resources and Demand of Customers

To model the variations in the output power of scattered wind products, the information received about wind speed (v) is used to model the probability density function (PDF) of a wind turbine. Rayleigh probability density function is used to model wind speed. This function for wind speed variations can be calculated by the following formula:

$$PDF(v) = \left(\frac{v}{sf^2}\right).exp\left[-(\frac{v^2}{2sf^2})\right] \quad (1)$$

In this formula, v and sf are wind speed and scale parameters, respectively. The relationship between wind turbine production capacity and wind speed is as follows:

$$\mathrm{P}_{wtg}(v(t)) = \begin{cases} 0 & , \quad v(t) < \mathrm{v}_{ci} \\ \dfrac{v(t) - v_{ci}}{v_r - v_{ci}} * P_r, & \mathrm{v}_{ci} < v(t) < \mathrm{v}_r \\ \mathrm{P}_r & , \quad \mathrm{v}_r < v(t) < \mathrm{v}_{co} \\ 0 & , \quad v(t) > \mathrm{v}_{co} \end{cases} \quad (2)$$

Where, P_r is the allowable power, v_{ci} is the cut-in speed, v_{co} is the cut-out speed, P_{wtg} is the output power of the wind turbine.

The hourly distribution of the emitted radiation is usually a bimodal distribution that can be considered as a linear combination of two distribution functions. To model the variations in the sun's radiation, the beta probability density function is used according to the following relation:

$$PDF(\beta) = \begin{cases} \dfrac{\Gamma(\alpha+\beta)}{\Gamma(\alpha)\cdot\Gamma(\beta)} \cdot \varphi^{(\alpha-1)} * (1-\varphi)^{\beta-1} & 0\le\varphi\le1,\ \alpha\ge0,\ \beta\ge0 \\ 0 & otherwise \end{cases} \quad (3)$$

The functional parameters of beta distribution (β and α) are calculated based on the mean (μ) and standard deviation (σ) of random variables according to the following equation:

$$\beta = (1-\mu) * (\frac{\mu*(1+\mu)}{\sigma^2} - 1) \quad (4)$$

$$\alpha = \frac{\mu*\beta}{1-\mu} \quad (5)$$

The uncertainty of the load is also considered as random variables whose prediction error is modeled using the normal probability density function. In this study, for the uncertainty model of each random variable, a set of possible scenarios is generated based on the Metropolis-Hastings algorithm and using the corresponding PDF. Then the scenarios generated by the k-means clustering method are reduced to an optimal subset, which indicates sufficient uncertainty. Finally, scenarios (wind, solar, and load) are combined to create complete sets based on the scenario tree. Each branch in the scenario tree corresponds to a scenario on the planning horizon with probability π_s, which is calculated as follows:

$$\pi_s = \pi_{k\_s} * \pi_{i\_s} * \pi_{l\_s} \quad (6)$$

Where, π_{l_s} , π_{i_s} , π_{k_s} are the probability of l_s-th load scenario, i_s-th PV scenario, and k_s-th wind scenario, respectively.

2.3. Objective Functions

Four main goals are considered in the proposed management plan. In other words, the proposed model is an optimal multi-objective operation model. These four goals are as follows:

1) Economic Objective function (ECOF)
   - Minimizing the cost of energy supply and reserving required micro-grid load and the energy cost required for electric vehicles on the planning horizon with the participation of responsive loads and charge and discharge management of electric vehicles

2) Security Objective function (SOF)
   - Minimizing bus voltage deviations from the nominal value on the planning horizon
   - Minimizing the deviation of the micro-grid frequency from the nominal value on the planning horizon
3) Environmental Objective function (EOF)
   - Minimizing greenhouse gas emissions on the planning horizon
4) Reliability Objective function (ROF)
   - Minimizing the lost load on the planning horizon

The mathematical model of the objective function is expressed as the following relation:

$$OF: \min[\ \omega_1\{ECOF\} + \omega_2\{SOF\} + \omega_3\{EOF\} + \omega_4\{ROF\}] \quad (7)$$

ω_1, ω_2, ω_3 and ω_4 are the weight coefficients of each of the system's objective functions. These coefficients make it possible to align the objective functions and also allow the operator to change the effectiveness of each objective function in the overall objective function of the system according to the priority in the operation. Each of the higher priority objective functions is multiplied by the larger weight factor.

For the variations in each component of the objective function to be equal (the importance of all components of the objective function is the same), the distance between the minimum and maximum value of each component of the objective function must be calculated and then the weights of the objective function are calculated in such a way that the distance between the minimum and maximum values of all sections is equal. If the minimum and maximum value of each component of the objective function is determined by the min and max indices, then the relationship between the weight coefficients is obtained from the following equations:

$$\frac{\omega_1}{\omega_2} = \frac{ECOF^{max} - ECOF^{min}}{SOF^{max} - SOF^{min}} \quad (8)$$

$$\frac{\omega_1}{\omega_3} = \frac{ECOF^{max} - ECOF^{min}}{EOF^{max} - EOF^{min}} \quad (9)$$

$$\frac{\omega_1}{\omega_4} = \frac{ECOF^{max} - ECOF^{min}}{ROF^{max} - ROF^{min}} \quad (10)$$

The variables and Indices of the objective functions are given in table 1.

Table 1. Variables and Indices of the objective functions.

Index of scenarios, buses, time periods and load groups	s, n, t, l
Index of wind, solar and DGs	k, i, j
Number of scenarios, buses, time periods and load groups	N_s, N_B, N_T, N_L
Number of wind, solar and DGs units	N_k, N_I, N_J
The scheduled power of the electric vehicle e to participate in V2G in the period t	$P_{e,t}^{EV}$
The scheduled active power of the DG j in the period t (and scenario s)(kw)	$P_{j,t}(P_{j,t,s})$
The scheduled reactive power of the DG j in the period t (and scenario s)(kvar)	$Q_{j,t}(Q_{j,t,s})$
The scheduled active power of the wind unit k in the period t (and scenario s)(kw)	$P_{k,t}(P_{k,t,s})$
The scheduled reactive power of the wind unit k in the period t (and scenario s)(kvar)	$Q_{k,t}(Q_{k,t,s})$
The scheduled active power of the solar unit i in the period t (and scenario s)(kw)	$P_{i,t}(P_{i,t,s})$
The scheduled reactive power of the solar unit i in the period t (and scenario s)(kvar)	$Q_{i,t}(Q_{i,t,s})$
The scheduled non-spinning reserve of the DG j in the period t (kw)	$R_{j,t}^{NS}$
The scheduled up-spinning reserve of the DG j (load l) in the period t (kw)	$R_{j,t}^{U}(R_{l,t}^{U})$
The scheduled down-spinning reserve of the DG j (load l) in the period t (kw)	$R_{j,t}^{D}(R_{l,t}^{D})$
The deployed non-spinning reserve of the DG j in the period t and scenario s (kw)	$r_{j,t,s}^{NS}$
The deployed up-spinning reserve of the DG j (load l) in the period t and scenario s (kw)	$r_{j,t,s}^{U}(r_{l,t,s}^{U})$
The deployed down-spinning reserve of the DG j (load l) in the period t and scenario s (kw)	$r_{j,t,s}^{D}(r_{l,t,s}^{D})$
Active(reactive) demand for load l in the period t (kw) (kvar)	$P_{l,t}(Q_{l,t})$
Active (reactive) power passing from bus n to bus m in period t (kW) (kVar)	$P_{n,m,t}(Q_{n,m,t})$

The binary variable, equal 1 if unit j is starting up in the period t (and scenario s)	$a_{j,t}(a_{j,t,s})$
The binary variable, equal 1 if unit j is shut down in the period t (and scenario s)	$b_{j,t}(b_{j,t,s})$
The binary variable, equal 1 if unit j is scheduled to be committed in the period t (and scenario s)	$u_{j,t}(u_{j,t,s})$
The bid price of electric vehicle e to participate in V2G in the period t (cent/kwh)	$\tau_{e,t}$
Electricity price for load l in period t (cent/kwh)	$\tau_{l,t}$
Energy bid submitted by wind unit k in period t (cent/kwh)	$\tau_{k,t}$
Energy bid submitted by solar unit i in period t (cent/kwh)	$\tau_{i,t}$
Cost function coefficients of DG j	A_j , B_j
The startup cost of DG j (cent)	SUC_j
Shutdown cost of DG j (cent)	SDC_j
The bid of the up (down)-spinning reserve submitted by DG j in period t (cent/kwh)	$(\tau_{j,t}^{R\_D})\tau_{j,t}^{R\_U}$
The bid of the up (down)-spinning reserve submitted by load l in period t (cent/kwh)	$(\tau_{l,t}^{R\_D})\tau_{l,t}^{R\_U}$
The bid of the non-spinning reserve submitted by DG j in period t(cent/kwh)	$\tau_{j,t}^{R\_NS}$
Real-time price for buying and selling deviation power from load l (EV e)(unit x)(cent/kwh)	$\tau'_{l,t}(\tau'_{x,t})(\tau'_{e,t})$
The amount of CO2, NOx and SO2 pollutants (per kg) produced per production of 1kWh of energy per unit of DG j	, α_{NOx}^{j}, $\alpha_{SO2}^{j}\alpha_{CO2}^{j}$
Load shedding of l-th load group in period t and scenario s (kw)	$P_{l,t,s}^{shed}$

2.3.1. Economic objective function

The economic objective function is intended to minimize the overall cost of MGO on the energy planning and reservation planning horizon. The overall cost of MGO includes energy supply and reservation costs to supply micro-grid electricity, participation fee for electric vehicles as V2G, and also expected operating costs under uncertainty. MGO income is the income from selling energy to customers. In this regard, the economic objective function of the system includes three main sets. These three sets include the planned MGO cost (F_1), the realized MGO cost (F_2), and the expected MGO income (F_3). Initially, energy distribution in the micro-grid is planned according to the mean load values and the production of renewable resources; then, according to each scenario and the difference between the amount of production and consumption with the predicted amount (average value), the final economic objective function is settled. Therefore, the economic objective function is expressed as follows:

$$ECOF = F_1 - F_2 - F_3 \tag{11}$$

The mathematical model of the F_1 set in the economic objective function of the system is expressed as follows:

$$F_1 = \sum_{t=1}^{N_T}\left[\begin{array}{l}\sum_{e=1}^{N_E}\tau_{e,t}.P_{e,t}^{EV} + \\ \sum_{j=1}^{N_J}[(A_j.u_{j,t} + B_j.P_{j,t}) + SUC_j.a_{j,t} + SDC_j.b_{j,t})] \\ + \sum_{j=1}^{N_J}[(\tau_{j,t}^{R\_D}.R_{j,t}^{D} + \tau_{j,t}^{R\_U}.R_{j,t}^{U} + \tau_{j,t}^{R\_NS}.R_{j,t}^{NS})] \\ + \sum_{l=1}^{N_L}[(\tau_{l,t}^{R\_D}.R_{l,t}^{D} + \tau_{l,t}^{R\_U}.R_{l,t}^{U})] \\ + \left[\sum_{k=1}^{N_K}\tau_{k,t}.P_{k,t} + \sum_{i=1}^{N_I}\tau_{i,t}.P_{i,t}\right]\end{array}\right] \tag{12}$$

The first part (F_{11}) is the cost paid by MGO for the V2G power programmed for electric vehicles. Electric vehicles are owned by customers.

$$F_{11} = \sum_{t=1}^{N_T}\sum_{e=1}^{N_E}\tau_{e,t}.P_{e,t}^{EV} \tag{13}$$

The second part (F_{12}) is the production cost of DG units and the cost of start-up and shutting them down according to the plan for the day ahead.

$$F_{12} = \sum_{t=1}^{N_T}\sum_{j=1}^{N_J}[(A_j.u_{j,t} + B_j.P_{j,t}) + SUC_j.a_{j,t} + SDC_j.b_{j,t})] \tag{14}$$

The third section (F_{13}) describes the reservation costs planned for production units.

$$F_{13} = \sum_{t=1}^{N_T}\sum_{j=1}^{N_J}[(\tau_{j,t}^{R\_D}.R_{j,t}^{D} + \tau_{j,t}^{R\_U}.R_{j,t}^{U} + \tau_{j,t}^{R\_NS}.R_{j,t}^{NS})] \quad (15)$$

The fourth section (F_{14}) describes the reservation costs planned by the load according to the DR program.

$$F_{14} = \sum_{t=1}^{N_T}\sum_{l=1}^{N_L}[(\tau_{l,t}^{R\_D}.R_{l,t}^{D} + \tau_{l,t}^{R\_U}.R_{l,t}^{U})] \quad (16)$$

The fifth section (F_{15}) represents the energy cost that buys MGO from owners of solar (PV) and wind (WT) units. In this study, it is assumed that PV and WT units are not owned by MGO. That is why WT and PV sell their energy to MGO at specific prices.

$$F_{15} = \sum_{t=1}^{N_T}\left[\sum_{k=1}^{N_K}\tau_{k,t}.P_{k,t} + \sum_{i=1}^{N_I}\tau_{i,t}.P_{i,t}\right] \quad (17)$$

As explained, in the second set of the economic objective function (F_2), according to the values of each scenario and the probability of occurrence of each scenario, the difference between the planned amount and the amount realized by the production units, loads, and renewable resources is settled. The mathematical model of the F_2 set in the economic objective function of the system is expressed as follows:

$$F_2 = \sum_{s=1}^{N_s}\sum_{t=1}^{N_T}\pi_s.\left[\begin{array}{l}\sum_{j=1}^{N_J} SUC_j.(a_{j,t,s} - a_{j,t}) + SDC_j.(b_{j,t,s} - b_{j,t}) + \\ \sum_{j=1}^{N_J}\tau'_{j,t}(r_{j,t,s}^{U} + r_{j,t,s}^{NS} - r_{j,t,s}^{D}) + \sum_{j=1}^{N_J}\tau'_{j,t}(r_{j,t,s}^{U} - r_{j,t,s}^{D}) \\ + \sum_{k=1}^{N_K}\tau'_{k,t}.\Delta P_{k,t,s} + \sum_{i=1}^{I}\tau'_{i,t}.\Delta P_{i,t,s} + \sum_{e=1}^{N_E}\tau'_{e,t,s}.\Delta P_{e,t,s}^{EV}\end{array}\right] \quad (18)$$

According to the above relation, F_2 consists of four parts. In the first part (F_{21}), the cost of commitment units in different scenarios is settled in real-time.

$$F_{21} = \sum_{s=1}^{N_s}\sum_{t=1}^{N_T}\sum_{j=1}^{N_J}\pi_s.[SUC_j.(a_{j,t,s} - a_{j,t}) + SDC_j.(b_{j,t,s} - b_{j,t})] \quad (19)$$

In the second part (F_{22}), according to the amount of achieved reservation, the cost of the commitment of DGs and responsive loads for network reservation is settled by the production units and customers who have participated in the DR program.

$$F_{22} = \sum_{s=1}^{N_s}\sum_{t=1}^{N_T}\pi_s.[(\sum_{j=1}^{N_J}\tau'_{j,t}(r_{j,t,s}^{U} + r_{j,t,s}^{NS} - r_{j,t,s}^{D}) + \sum_{j=1}^{N_J}\tau'_{j,t}(r_{j,t,s}^{U} - r_{j,t,s}^{D})] \quad (20)$$

In the third section (F_{23}), the energy supply costs are settled by the PV and WT units, which are the result of the difference between the real-time output power and the predicted power for the coming day.

$$F_{23} = \sum_{s=1}^{N_s}\sum_{t=1}^{N_T}\pi_s.[\sum_{k=1}^{N_K}\tau'_{k,t}.\Delta P_{k,t,s} + \sum_{i=1}^{I}\tau'_{i,t}.\Delta P_{i,t,s}] \quad (21)$$

It should be noted that in the first stage of programming, MGO considers WT and PV units based on the predicted values in the programming, but due to the changing weather conditions, the output power of these units always changes. Therefore, in section F_{23}, the cost exchanged by the owners of PV and WT units should be paid based on the difference between actual and predicted production in each scenario. This component can be positive or negative on the planning horizon.

In the fourth section (F_{24}), the cost of paying customers in real-time is settled according to the amount of power realized for the participation of electric vehicles in V2G mode.

$$F_{24} = \sum_{s=1}^{N_s}\sum_{t=1}^{N_T}\pi_s.[\sum_{e=1}^{N_E}\tau'_{e,t,s}.\Delta P_{e,t,s}^{EV}] \quad (22)$$

Finally, the third set of the economic objective function (F_3) indicates MGO income from electricity sales to customers. This income is determined by the net consumption of the customers (the predicted average value) and the price of electricity per hour.

$$F_3 = \sum_{t=1}^{N_T}\sum_{l=1}^{N_L}\tau_{l,t}.P_{l,t} \quad (23)$$

2.3.2. Security objective Function

In the third objective function of the system, the optimization approach is based on minimizing the

deviations of the bus voltage and the frequency deviation of the micro-grid from the nominal value. The voltage of the buses and the frequency of the micro-grid are also calculated based on the droop control relations. Relationships related to frequency and voltage droop control are expressed in reference [18].

$$SOF = \sum_{s=1}^{N_S}\sum_{t=1}^{N_T}\pi_s.\left[\left|f_{t,s} - f^{ref}\right| + \sum_{n=1}^{N_B}\left|V_{n,t,s} - V^{ref}\right|\right] \quad (24)$$

In the above relation, V^{ref} is the value of the nominal voltage in the n-th bus and f^{ref} is the value of the nominal frequency of the micro-grid.

2.3.3. Environmental objective function

In order to consider the destructive effects of environmental pollution caused by pollutants produced by various energy sources, the third objective function of the optimization problem is considered as the total emission of micro-grids, along with other objective functions. This is done to pay more attention to renewable energy-based dispersed products. In this objective function (EOF), the most common environmental pollutants include sulfur dioxide (SO_2), nitrogen oxides (NO_x) and carbon dioxide (CO_2), which are considered. This objective function includes the penalty for emitting pollutants produced by non-renewable distributed products and is calculated as follows:

$$EOF = \sum_{s=1}^{N_S}\sum_{t=1}^{N_T}\pi_s(\sum_{j=1}^{N_J}P_{j,t,s}.(\alpha_{CO2}^{j}k_{CO2} + \alpha_{NOx}^{j}k_{NOx} + \alpha_{SO2}^{j}k_{SO2}) \quad (25)$$

According to the above relationship, the amount of this fine depends on the production capacity of non-renewable units. This part of the objective function leads the operator to maximize the use of renewable energy sources. Since pollutants NO_x and SO_2 are more harmful than CO_2, this has been addressed in the model by setting the weight coefficients (k_{SO2}‘k_{CO2}‘ k_{NOx}). The values of these coefficients are determined according to the reference [19].

2.3.4. Reliability objective function

The fourth objective function is intended to increase the reliability of the power supply. In this objective function, the Expected Energy Not Supplied (EENS) for non-elastic loads is expressed in different scenarios.

$$ROF = \sum_{j=1}^{N_j} VOLL.EENS_j \quad (26)$$

The value of EENS for customer l during the planning horizon is formulated as follows:

$$EENS_j = \sum_{t=1}^{N_T}\sum_{s=1}^{N_S}\pi_s\,.P_{l,t,s}^{shed} \quad (27)$$

2.4. Restrictions

The limitations of the proposed plan are as follows:

2.4.1. AC load flow constraint in micro-grid

As explained in the previous section, in a micro-grid, the frequency and voltage are controlled by active and reactive power. In other words, an imbalance between production and consumption power affects the frequency and voltage of the micro-grid. Therefore, the AC load flow is required to calculate the voltage and frequency deviation in the absence of an infinite bus. The equations for the equilibrium of active and reactive power at time t in each of the micro-grid buses in the steady-state are defined as follows:

$$\sum_{j:(j,n)\in J(t)}P_{j,t} + \sum_{k:(k,n)\in K(t)}P_{k,t} + \sum_{i:(i,n)\in I(t)}P_{i,t} - \sum_{l:(l,n)\in L(t)}P_{l,t} = \sum_{m:(n,m)\in B(t)}P_{n,m,t} \quad (28)$$

$$\sum_{j:(j,n)\in J(t)}Q_{j,t} + \sum_{k:(k,n)\in K(t)}Q_{k,t} + \sum_{i:(i,n)\in I(t)}Q_{i,t} - \sum_{l:(l,n)\in L(t)}Q_{l,t} = \sum_{m:(n,m)\in B(t)}Q_{n,m,t} \quad (29)$$

$P_{n,m,t}$ and $Q_{n,m,t}$ are the active and reactive power passing from bus n to bus m during the period t, which are calculated by the following relations:

$$P_{n,m,t} = G_{n.m}\left[V_{n,t}^2 - V_{n,t}\cdot V_{m,t}\cos(\delta_{n,t} - \delta_{m,t})\right] - B_{n,m}V_{n,t} \cdot V_{m,t}\sin(\delta_{n,t} - \delta_{m,t}) \quad (30)$$

$$Q_{n,m,t} = -B_{n,m}\left[V_{n,t}^2 - V_{n,t} \cdot V_{m,t}\cos(\delta_{n,t} - \delta_{m,t})\right] - G_{n,m}V_{n,t} \cdot V_{m,t}\sin(\delta_{n.t} - \delta_{m,t}) \quad (31)$$

Where, $V_{n,t}$ and $V_{m,t}$, are n node and m node voltage at time t, respectively, $G_{n,m}$ and $B_{n,m}$ are the line conductance and susceptance between n and m nodes and $\delta_{n,t}$, $\delta_{m,t}$ are also the voltage angles of node n and node m at time t in rad.

Depending on the random model, operational and technical constraints must be established in each of the system scenarios. So we have:

$$\sum_{j:(j,n)\in J(t,s)} P_{j,t,s} + \sum_{k:(k,n)\in K(t,s)} P_{k,t,s} + \sum_{i:(i,n)\in I(t,s)} P_{i,t}, s - \sum_{l:(l,n)\in L(t,s)} P_{l,t,s} = \sum_{m:(n,m)\in B(t,s)} P_{n,m,t,s} \quad (32)$$

$$\sum_{j:(j,n)\in J(t,s)} Q_{j,t,s} + \sum_{k:(k,n)\in K(t,s)} Q_{k,t,s} + \sum_{i:(i,n)\in I(t,s)} Q_{i,t}, s - \sum_{l:(l,n)\in L(t,s)} Q_{l,t,s} = \sum_{m:(n,m)\in B(t,s)} Q_{n,m,t,s} \quad (33)$$

$$P_{n,m,t,s} = G_{n,m}\left[V_{n,t,s}^2 - V_{n,t,s} \cdot V_{m,t,s}\cos(\delta_{n,t,s} - \delta_{m,t,s})\right] - B_{n,m}V_{n,t,s} \cdot V_{m,t,s}\sin(\delta_{n,t,s} - \delta_{m,t,s}) \quad (34)$$

$$Q_{n,m,t,s} = -B_{n,m}\left[V_{n,t,s}^2 - V_{n.t.s} \cdot V_{m,t,s}\cos(\delta_{n,t,s} - \delta_{m,t,s})\right] - G_{n,m}V_{n,t,s} \cdot V_{m,t,s}\sin(\delta_{n,t,s} - \delta_{m,t,s}) \quad (35)$$

2.4.2. Distributed generation restrictions

There are operation restrictions to distributed generations that must be considered in the planning process. In the following, several relationships between the production capacity of distributed generation units and incremental and decreasing reservations have been expressed as system adjustment capacities.

$$P_j^{min}u_{j,t} + R_{j,t}^D \le P_{j,t} \le P_j^{max}u_{j,t} - R_{j,t}^U \quad (36)$$

$$0 \le R_{j,t}^U \le R_{j,t}^{U,max}\, u_{j,t} \quad (37)$$

$$0 \le R_{j,t}^D \le R_{j,t}^{D,max}\, u_{j,t} \quad (38)$$

$$0 \le R_{j,t}^{NS} \le R_{j,t}^{NS.max}\,(1 - u_{j,t}) \quad (39)$$

Relationship (36) indicates the minimum and maximum power of DGs. In relation (37) to (39), the range of the planned up-spinning reserve, down-spinning reserve, and non-spinning reserve for unit j at time t are specified, respectively. In these relationships, P_j^{min} is the minimum and P_j^{max} is the maximum output of DG j. $R_{j,t}^{U,max}$ and $R_{j,t}^{D,max}$ are the maximum contribution of unit j in providing up-spinning and down-spinning reserves. $R_{j,t}^{NS.max}$ is the maximum contribution of unit j to the provision of the non-spinning reserve at time t.

In the random model, the relationship between the production capacity of the distributed generation units and the incremental and decremental reservations are expressed as the regulatory capacities of the system in each scenario in the following relationships:

$$P_j^{min}u_{j,t,s} + r_{j,t,s}^D \le P_{j,t,s} \le P_j^{max}u_{j,t,s} - r_{j,t,s}^U \quad (40)$$

$$0 \le r_{j,t,s}^U \le R_{j,t,s}^{U,max}\, u_{j,t,s} \quad (41)$$

$$0 \le r_{j,t,s}^D \le R_{j,t,s}^{D,max}\, u_{j,t,s} \quad (42)$$

$$0 \le r_{j,t,s}^{NS} \le R_{j,t,s}^{NS.max}\,(1 - u_{j,t,s}) \quad (43)$$

$$P_{j,t} = P_{j,t,s} + r_{j,t,s}^U + r_{j,t,s}^{NS} - r_{j,t,s}^D \quad (44)$$

$$Q_j^{min} \le Q_{j,t,s} \le Q_j^{max} \quad (45)$$

(44) shows the relationship between the programmed power of DGs and the reserve power (due to increased or decreased production) for each scenario. The relation (45) also shows the minimum Q_j^{min} and the maximum Q_j^{max} of the allowed reactive power for each unit in each scenario and for all the planning horizon times.

2.4.3. Restrictions and Equations of Frequency Security

When the micro-grid frequency deviates from the normal range value, the central controller must return the frequency to the nominal value, by resetting the distributed generation output settings or using the DR program. Besides, the restoration function must be in line with the economic goals of the micro-grid. Therefore, based on the droop control function of the distributed generations, the frequency in the steady-state can be formulated as follows:

$$f_{t,s} = -\sum_{j}^{N_J}\left(P_{j,t,s} - P_{j,t,s}^{ref}\right) \Big/ \left[D_{l,t,s} + \sum_{j}^{N_J}\left(\frac{1}{m_{p,j}}\right)u_{j,t}\right] \quad (46)$$

This relationship has been developed according to the droop control equation in reference [18]. $P_{j,t,s}^{ref}$ is the reference point of the production power for the DG j at time t and scenario s.

$D_{l,t,s}$ is the frequency elasticity of MG loads at period t and in scenario s. $m_{p,j}$ is the frequency droop coefficient, $f_{t,s}$ is the micro-grid frequency at time t and scenario s.

To keep the frequency stable, the MGCC must adjust the active power of the distributed generation units to achieve the following criteria. To ensure that frequency deviations are within an acceptable range, micro-grid frequency deviations must be less than the allowable frequency deviations. So we have:

$$\left|\Delta f_{t,s}\right| \le \Delta f^{max} \quad (47)$$

In this relation, Δf^{max} is the maximum allowable amount of microgrid frequency deviation.

2.4.4. Technical limitations of the network

In addition to the stated constraints, the following relations are the constraints of the node voltage limit and the power limit of the lines.

$$V^{min} \le V_{n,t,s} \le V^{max} \quad (48)$$

$$\sqrt{(P_{n,m,t,s})^2 + (Q_{n,m,t,s})^2} \le S_{n,m}^{max} \quad (49)$$

In the above relations, V^{max} and V^{min} are the maximum and minimum allowable value of voltage for bus n in scenario s and period t. $P_{n,m}^{max}$ is also the maximum power passing through the connecting line between bus n and bus m.

2.4.5. Restrictions and equations of electric vehicles

The data on the time of entry and exit of electric vehicles depends on the behavior of the owners of electric vehicles. According to reference [20], the management of electric vehicles is based on the following three assumptions:

- Electric vehicles are connected to the grid in household parking lots for charging or discharging. In other words, electric vehicles are in the place of customers and load buses.
- After daily use, electric vehicles return to the parking lot and connect to the grid.
- Electric vehicles are connected to the network only once a day and are ready to be charged or discharged. In other words, the frequent connection of vehicles during the day has been omitted.

Electric vehicle restrictions are divided into the following three categories:

- Limit the power of vehicle exchanges with the network
- Technical limitation of the vehicle battery
- Energy limit on the vehicle battery

The rate of change in the battery charge percentage of the electric vehicle e at time t is calculated by the following equation:

$$SOC_{e,t}^{EV} = SOC_{e,t-1}^{EV} - \frac{1}{C_e^{max}}\left(\frac{1}{1-P_{e,t}^{L\_V2G}}\cdot\frac{1}{\eta_e^{BTB}}\cdot P_{e,t}^{V2G} - \left(1 - P_{e,t}^{L\_G2V}\right)\cdot P_{e,t}^{G2V}\cdot\eta_e^{BTB}\right) \quad (50)$$

In the above relation, e is the index of the electric vehicle. C_e^{max} is the battery capacity of the electric vehicle e. $P_{e,t}^{L\_V2G}$ and $P_{e,t}^{L\_G2V}$ are the losses in V2G (discharge) and G2V (charge) mode for electric vehicle e, respectively. $P_{e,t}^{V2G}$ and $P_{e,t}^{G2V}$ are the power exchanged between the network and the electric vehicle e at time t in the V2G (discharge) and G2V (charge) mode. η_e^{BTB} is the converter efficiency between the vehicle e and the network. $SOC_{e,t-1}^{EV}$ is the initial charge value of the electric vehicle e. The initial value for the first SOC ($SOC_{e,t=1}^{EV}$) is equal to the last SOC status in the last period of the previous day.

Given that the maximum amount of EV charge is 100%, so we have for each vehicle:

$$0 \le SOC_{e,t}^{EV} \le 1 \quad (51)$$

The amount of power exchange between the vehicle and the network for EV e and at time t is limited by the vehicle's battery capacity (C_e^{max}) and vehicle charge percentage ($SOC_{e,t-1}^{EV}$). To show the charge and discharge state of the electric vehicle e at time t, the binary variable $X_{e,t}^{EV}$ is considered.

$$0 \le P_{e,t}^{G2V} \le C_e^{max}\left(1 - SOC_{e,t-1}^{EV}\right).\frac{1}{1-P_{e,t}^{L_G2V}}.\frac{1}{\eta_e^{BTB}}.\left(1 - X_{e,t}^{EV}\right) \quad (52)$$

$$0 \le P_{e,t}^{V2G} \le C_e^{max}.SOC_{e,t-1}^{EV}.\left(1 - P_{e,t}^{Lv2G}\right).\eta_e^{BTB}.X_{e,t}^{EV} \quad (53)$$

$$P_{e,t}^{EV} = B_{e,t}^{EV} - P_{e,t}^{LE} \quad (54)$$

$B_{e,t}^{EV}$ is the power exchange between the vehicle battery and charger/discharge converter (converter input) and $P_{e,t}^{EV}$ is the Power exchange between network and charge/discharge converter and $P_{e,t}^{LE}$ is the loss of charge/discharge converter for the vehicle e in the period t.

As explained above, the power exchanged between the vehicle and the network ($P_{e,t}^{EV}$), if the electric vehicle is in the charging state (G2V), as $P_{e,t}^{G2V}$ and if it is in the discharge state (V2G) as $P_{e,t}^{V2G}$. Therefore, the following relationship is established for each vehicle in each hour:

$$P_{e,t}^{EV} = P_{e,t}^{G2V} - P_{e,t}^{V2G} \quad (55)$$

The limitations for energy balance in an electric vehicle are as follows:

$$W_{e,t=1}^{EV} = W_{e,0}^{EV} + B_{e,t=1}^{EV} \quad (56)$$

$$W_{e,t}^{EV} = W_{e,t-1}^{EV} + B_{e,t}^{EV} \quad (57)$$

In other words, the energy stored in the battery is equal to the primary energy in the battery (when the vehicle is connected to the network) plus the exchange energy with the network.

2.4.6. Limitations and equations of the demand response program

Responsive load management, along with electric vehicles, has been proposed in this model to improve micro-grid performance, especially during peak load times. This management plan expresses the behavior of the load in response to incentives and uses it to improve network operation. In this model, the responsive loads are modeled as follows:

- Price-sensitive loads
- Voltage-sensitive loads
- Frequency-sensitive loads

Since the location of customers in the micro-grid and the level of their participation in the DR, and the program is different, so customers in the N_L -group are classified with the participation of γ_l . Customers participating in the DR program change their consumption pattern based on electricity price signals and the amount of voltage and frequency deviation from the nominal value. Therefore, the total load demand of the system after participating in the DR program in the period t is calculated as follows:

$$D_t = \sum_{l=1}^{N_L} [P_{l,t}^{NDR} + P_{l,t}^{DR}] \quad (58)$$

In this regard, $P_{l,t}^{NDR}$ and $P_{l,t}^{DR}$ are the non-responsive loads and the responsive loads in the l group of customers, respectively. To maximize benefits, each customer group may change their load level from $P_{l,t}$ to $P_{l.t}^{DR}$ in time t. So we have:

$$\Delta P_{l,t}^{DR} = P_{l,t} - P_{l.t}^{DR} \quad (59)$$

$\Delta P_{l,t}^{DR}$ shows the rate of change in customer load due to participation in the DR program. According to the reference [21], the elasticity ($E_{l,t,v}$) and customer participation in the price-sensitive demand response program ($P_{l.t}^{DR-\tau}$) are calculated as follows. The benefits of Group l customers by participating in the price-sensitive DR program can be calculated as follows:

$$B(P_{l.t}^{DR-\tau}) = I(P_{l.t}^{DR-\tau}) - P_{l.t}^{DR-\tau}.\tau_{l,t} \quad (60)$$

$\tau_{l,t}$ is the price of electricity to supply load l therefore $P_{l.t}^{DR-\tau}.\tau_{l,t}$ is the amount paid by the customers to supply the load $P_{l.t}^{DR-\tau}$. $I(P_{l.t}^{DR-\tau})$ is the customer income from participating in DR and $B(P_{l.t}^{DR-\tau})$ is the benefit of the customer's group l in the period t after the implementation of the price-sensitive DR program. To maximize the benefit of l group customers, we derive the relation (60) from $P_{l.t}^{DR-\tau}$. So we have:

$$\frac{\partial B(P_{l.t}^{DR-\tau})}{\partial P_{l.t}^{DR-\tau}} = \frac{\partial I(P_{l.t}^{DR-\tau})}{\partial P_{l.t}^{DR-\tau}} - \tau_{l,t} = 0 \Rightarrow \frac{\partial I(P_{l.t}^{DR-\tau})}{\partial P_{l.t}^{DR-\tau}} = \tau_{l,t} \quad (61)$$

Momentary variations in demand to price variations at the same time are defined as self-elasticity ($E_{l,t,t}^{\tau}$) and is defined in mathematical language as follows:

$$E_{l,t,t}^{\tau} = \frac{\tau_{l,t}^0}{P_{l,t}^0} . \frac{\partial P_{l,t}}{\partial \tau_{l,t}} \quad (62)$$

According to Equation (62) and based on the quadratic-order DR model, the income of l group customers in the period t after using the price-sensitive DR program is calculated by the following equation:

$$I(P_{l.t}^{DR-\tau}) = I_{l,t}^0 + \frac{\tau_{l,t}^0 . P_{l,t}^{DR-\tau}}{1 + (E_{l,t,t}^{\tau})^{-1}} * \left[(\frac{P_{l,t}^{DR-\tau}}{P_{l,t}})^{(E_{l,t,t}^{\tau})^{-1}} - 1 \right] \quad (63)$$

Derivation from (63) leads to

$$\frac{\partial I(P_{l,t}^{DR-\tau})}{\partial P_{l,t}^{DR-\tau}} = \frac{\tau_{l,t}^{0}}{1+(E_{l,t,t}^{\tau})^{-1}} * \left[\left(\frac{P_{l,t}^{DR-\tau}}{P_{l,t}}\right)^{(E_{l,t,t}^{\tau})^{-1}} - 1\right] + \frac{\tau_{l,t}^{0}.\ P_{l,t}^{DR-\tau}}{1+(E_{l,t,t}^{\tau})^{-1}} * \left[(E_{l,t,t}^{\tau})^{-1}.\frac{1}{P_{l,t}}\left(\frac{P_{l,t}^{DR-\tau}}{P_{l,t}}\right)^{(E_{l,t,t}^{\tau})^{-1}-1}\right] \quad (64)$$

Placing (64) in (62) gives

$$(E_{l,t,t}^{\tau})^{-1}+1) * \frac{\tau_{l,t}^{0}}{\tau_{l,t}} = \left(\frac{P_{l,t}^{DR-\tau}}{P_{l,t}}\right)^{(E_{l,t,t}^{\tau})^{-1}} - 1 + (E_{l,t,t}^{\tau})^{-1}.\left(\frac{P_{l,t}^{DR-\tau}}{P_{l,t}}\right)^{(E_{l,t,t}^{\tau})^{-1}} \quad (65)$$

$$\Longrightarrow \frac{\tau_{l,t}}{\tau_{l,t}^{0}} = \left(\frac{P_{l,t}^{DR-\tau}}{P_{l,t}}\right)^{(E_{l,t,t}^{\tau})^{-1}} - \frac{1}{1+(E_{l,t,t}^{\tau})^{-1}}$$

Therefore, the amount of l group demand at time t is obtained from the following equation:

$$P_{l,t}^{DR-\tau} = P_{l,t}.\left(\frac{\tau_{l,t}^{0}}{\tau_{l,t}} + \frac{1}{1+(E_{l,t,t}^{\tau})^{-1}}\right)^{E_{l,t,t}^{\tau}} \quad (66)$$

In the same way, the cross-elasticity of price ($E_{l,t,v}^{\tau}$) means the sensitivity of demand l to price variations in the t-th period relative to price variations in the v-th period in the following mathematical language:

$$E_{l,t,v}^{\tau} = \frac{\tau_{l,t}^{0}}{P_{l,t}^{0}}.\frac{\partial P_{l,t}}{\partial \tau_{l,v}} \quad (67)$$

$\tau_{l,t}$ is the price of electricity for load l in the period v, $\tau_{l,t}^{0}$ is the initial price of electricity for the load l in the period v. Based on the quadratic-order DR model and according to (67), the responsive loads that must be transferred from other periods to period t are modeled using the following equations:

$$P_{l,t}^{DR-\tau} = P_{l,t}.\exp\left[\sum_{\substack{v=1\\v\neq t}}^{N_T} E_{l,t,v}^{\tau}.\ln\left(\frac{\tau_{l,v}}{\tau_{l,v}^{0}} + \frac{1}{1+(E_{l,t,v}^{\tau})^{-1}}\right)\right] \quad (68)$$

$$P_{l,t}^{DR-\tau} = P_{l,t}.\prod_{\substack{v=1\\v\neq t}}^{N_T}\left(\frac{\tau_{l,v}}{\tau_{l,v}^{0}} + \frac{1}{1+(E_{l,t,v}^{\tau})^{-1}}\right)^{E_{l,t,v}^{\tau}} \quad (69)$$

Therefore, the total demand of customers after participating in the price-sensitive DR program according to (66) and (69) is as follows:

$$P_{l,t}^{DR-\tau} = P_{l,t}.\prod_{v=1}^{N_T}\left(\frac{\tau_{l,v}}{\tau_{l,v}^{0}} + \frac{1}{1+(E_{l,t,v}^{\tau})^{-1}}\right)^{E_{l,t,v}^{\tau}}$$
$$\Rightarrow P_{l,t}^{DR-\tau} = P_{l,t}.\prod_{v=1}^{N_T}\exp\left[ln\left(\frac{\tau_{l,v}}{\tau_{l,v}^{0}} + \frac{1}{1+(E_{l,t,v}^{\tau})^{-1}}\right)^{E_{l,t,v}^{\tau}}\right] \quad (70)$$
$$\Rightarrow P_{l,t}^{DR-\tau} = P_{l,t}.\exp\sum_{v=1}^{N_T} E_{l,t,v}^{\tau}.\ln\left(\frac{\tau_{l,v}}{\tau_{l,v}^{0}} + \frac{1}{1+(E_{l,t,v}^{\tau})^{-1}}\right)$$

Finally, according to Equation (70), the price-sensitive load response model is as follows:

$$P_{l,t}^{DR-\tau} = P_{l,t}.\exp\sum_{v=1}^{N_T} E_{l,t,v}^{\tau}.\ln\left(\frac{\tau_{l,v}}{\tau_{l,v}^{0}} + \frac{1}{1+(E_{l,t,v}^{\tau})^{-1}}\right) \quad (71)$$

Similar to the process for the relationship (71), The demand response model sensitive to frequency variations ($P_{l,t}^{DR-f}$) and the demand response sensitive to voltage variations ($P_{l,t}^{DR-V}$) are also obtained according to relations (72) and (73), respectively:

$$P_{l,t}^{DR-f} = (P_{l,t} - P_{l,t}^{DR-\tau}).\exp\sum_{v=1}^{N_T} E_{l,t,v}^{f}.\ln\left(\frac{f_v}{f_v^{0}} + \frac{1}{1+\left(E_{l,t,v}^{f}\right)^{-1}}\right) \quad (72)$$

$$P_{l,t}^{DR-V} = \left(P_{l,t} - P_{l,t}^{DR-\tau} - P_{l,t}^{DR-f}\right).\exp\sum_{v=1}^{N_T} E_{l,t,v}^{f} \,.\, \ln\left(\frac{V_{l,v}}{V_{l,v}^{0}} + \frac{1}{1+\left(E_{l,t,v}^{v}\right)^{-1}}\right) \quad (73)$$

In the above relations, $E_{l,t,v}^{\tau}$ is the sensitivity of demand l to voltage variations in t-th of the time period relative to variations in voltage in v-th of the time period and $E_{l,t,v}^{f}$is the sensitivity of demand l to variations the frequency in t-th of the time period relative to the frequency variations in v-th of the time period. $V_{l,v}$ is the voltage of the node where the responsive load is located at v in v-th of the time period and f_v is the micro-grid frequency at the v-th of the time period. It should be noted that the price-sensitive demand response program is initially implemented. If there is more load capacity to participate in the demand response program, then the frequency- sensitive response program and finally the voltage-sensitive response program are implemented. By placing the relations (71), (72), and (73) in (58), the complete load response model is obtained as follows:

$$P_{l,t} = (1-\gamma_l)P_{l,t} + \gamma_l.\left[(P_{l,t}^{DR-\tau}.d_1) + (P_{l,t}^{DR-f}.d_2) + (P_{l,t}^{DR-V}.d_3)\right] \quad (74)$$

γ_l is the potential for implementing the DR program in load l. d_1, d_2 and d_3 are binary variables. If d_1, d_2 and d_3 are equal to 1, then the load is sensitive to price, frequency, and voltage respectively.

2.4.7. Load restrictions

Constraints (75) and (76) express the limitation of increasing and decreasing reserves on the demand side. Note that increasing or decreasing the reserve of the demand side means an increase or decrease in the level of customer's consumption.

$$0 \le r_{l,t,s}^{U} \le R_{l,t,s}^{U} \quad (75)$$

$$0 \le r_{l,t,s}^{D} \le R_{l,t,s}^{D} \quad (76)$$

$R_{l,t,s}^{U}$and $R_{l,t,s}^{D}$ are the amount of scheduled reserve and $r_{l,t,s}^{U}$and $r_{l,t,s}^{D}$ are the amount of Increasing and decreasing operational reserve for the l-th load at time t and scenario s. Theses constraints for both active and reactive loads are as follows:

$$P_{l,t}^{min} \le P_{l,t} \le P_{l,t}^{max} \quad (77)$$

$$0 \le R_{l,t}^{U} \le P_{l,t} - P_{l,t}^{min} \quad (78)$$

$$0 \le R_{l,t}^{D} \le P_{l,t}^{max} - P_{l,t} \quad (79)$$

$R_{l,t}^{U}$ and $R_{l,t}^{D}$ are the amount of incremental and decremental scheduled reserve for l group load at time t. (80) shows the relationship between the amount of scheduled load of customers and the considered reserved load (due to an increase or decrease of load) for each scenario.

$$P_{l,t} = P_{l,t,s} - r_{l,t,s}^{U} + r_{l,t,s}^{D} \quad (80)$$

$r_{l,t,s}^{D}$ and $r_{l,t,s}^{U}$ are the amount of time that is scheduled in time t and scenario s according to the DR program as a decrease or increase reservation.

2.4.8. Restriction of emergency shutdown

The following relationships describe the limitation of active and reactive emergency loads.

$$0 \le P_{l,t,s}^{shed} \le P_{l,t} \quad (81)$$

$$Q_{l,t,s}^{shed} = \tan\theta \,.\, P_{l,t,s}^{shed} \quad (82)$$

$P_{l,t,s}^{shed}$ Indicates the amount of active power outage (kW) in the non-flexible (non-elasticity) loads in the l group of the load times at time t and scenario s.

2.4.9. Piecewise Linear AC Power Flow

In the previous section, AC power flow constraints are nonlinear and must be linearized to fit the linear programming model. The following equations provide a linear approximation of the AC power flow in which voltage and reactive power are modeled.

$$P_{n,m,t,s} = G_{n,m}.\left[V_{n,t,s} - V_{m,t,s} - \omega_{n,m,t,s} + 1\right] - m(\delta_{n,t,s} - \delta_{m,t,s}) \quad (83)$$

$$Q_{n,m,t,s} = -B_{n,m}.\left[V_{n.t.s} - V_{m.t.s} + \omega_{n,m.t.s} + 1\right] - G_{n,m}.(\delta_{n,t,s} - \delta_{m,t,s}) \quad (84)$$

Over a typical range of voltage angle i.e., $\left|\delta_{n,t,s} - \delta_{m,t,s}\right| \le 10^{\circ}$, $\omega_{n,m.t.s}$ represents the piecewise linear approximation of $\cos\left(\delta_{n,t,s} - \delta_{m,t,s}\right)$ [22].

$$\omega_{n,m.t.s} = d_{n,m,t,s}.\left(\delta_{n,t,s} - \delta_{m,t,s}\right) + e_{n,m.t.s} \quad (85)$$

In the above relation, $d_{n,m.t.s}$ and $e_{n,m.t.s}$ are selected so that $\omega_{n,m.t.s}$ and $\cos(\delta_{n,t,s} - \delta_{m,t,s})$ intersect at the breakpoint. The approximation errors associated with this model can be found in [23].

3. SIMULATION AND NUMERICAL RESULTS

The micro-grid structure of the test is shown in Fig 1. The network is a low voltage network that consists of

several radial branches and is operated in island mode. On the production side, the micro-grid has five controllable distributed units, including two micro-turbines, two fuel cells and a gas generator, and three renewable units, including two solar panels and a wind turbine.

The information about the production units is given in Table 2. The recommended optimization time horizon is 24 hours. In order to model the uncertainties in the proposed model, based on the corresponding probability density functions, 2000 initial scenarios have been generated for the output power of wind and solar units and the participation rate of responsive loads.

Table 2 Technical information of distributed generations [1].

Title	A (cent/kWh)	B (cent/kWh)	SUC (cent)	SDC (cent)	P^{min} (kW)	P^{max} (kW)	τ^{R-U} (cent)	τ^{R-D} (cent)	τ^{R-NS} (cent)	Emission $(^{kg}/_{kWh})$	m_p
DG1	315.2	8.32	11.2	8	40	170	1.9	1.9	1.9	0.92	0.01
DG2	195.1	5.52	8.5	7	30	160	2.3	2.3	2.3	0.61	0.52
DG3	362.2	15.52	17.5	10	25	140	1.7	1.7	1.7	0.31	0.27
DG4	362.2	15.52	17.5	10	25	140	1.7	1.7	1.7	0.31	0.27
DG5	195.1	5.52	8.5	7	30	160	2.3	2.3	2.3	0.61	0.52

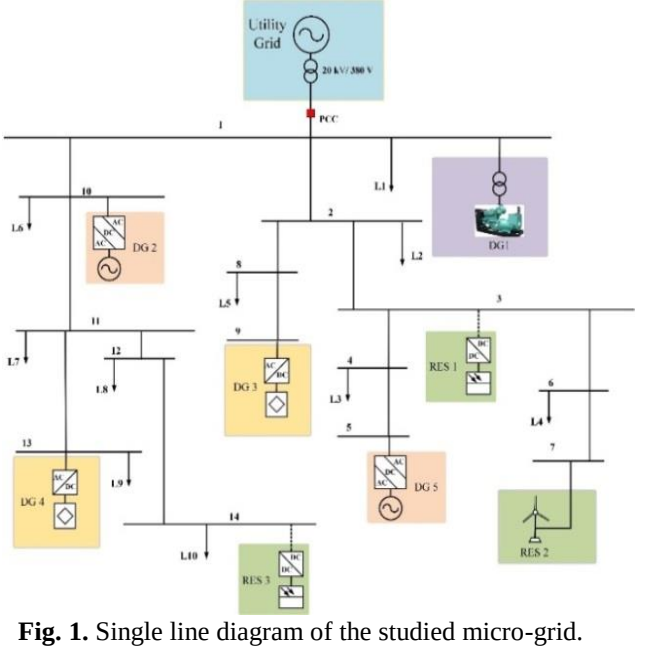

Fig. 1. Single line diagram of the studied micro-grid.

In the next step, by implementing the scenario reduction algorithm, the scenarios are reduced to 30 scenarios. Reduced scenarios are used to Mixed-Integer Linear Programming (MILP) to achieve maximum operating profit by ensuring voltage and frequency security. The optimization problem designed by the CPLEX algorithm has been solved in GAMS software. The predicted hourly output power for wind and solar units is also shown for various scenarios in Fig 2 and Fig 3. The power factor of the solar unit is assumed to be 1 and the power factor of the wind unit is 0.95.

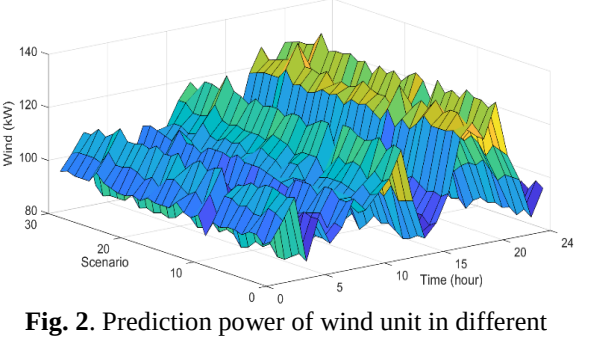

Fig. 2. Prediction power of wind unit in different scenarios.

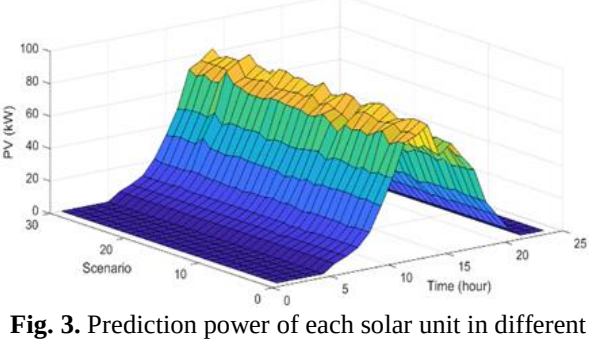

Fig. 3. Prediction power of each solar unit in different scenarios.

According to Fig 1, the micro-grid consists of 10 balanced three phases loads. The complete model of responsive load management (all three types of responsive loads sensitive to voltage, frequency, and price) has been applied in this network. The power factor of loads is assumed to be 0.95 lag. The loads are equally distributed between phases. The cost of up and down reserves on the load side is assumed to be 2.3 cents / kW and 1.9 cents / kW, respectively. The cost of producing

wind turbines and solar panels is 12.2 cents / kWh and 62.1 cents / kWh, respectively. The value of lost load (VOLL) is also assumed to be 1000 cents / kWh. The curve of total hourly variations in the total load of the micro-grid and the electricity tariff is shown in Fig 4 and Fig 5.

According to Fig 4, in this study, the load is divided into three periods: 1: 00-5: 00, low load period, 11:00-15:00 and 19: 00-22: 00, full load period, and 6: 00-10: 00 and 16: 00-18: 00 and 23: 00-00: 00 are considered the intermediate period. The rated voltage and frequency of the studied micro-grid are assumed to be 380V and 50HZ, respectively. The allowable deviation of bus voltage and micro-grid frequency is ± 10% and ± 1%, respectively.

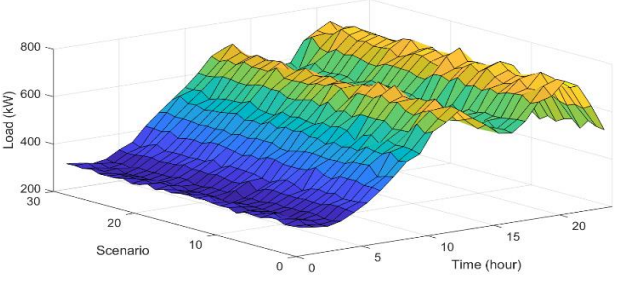

Fig. 4. Curve variations of the total load of the micro-grid in 24 hours of programming and different scenarios.

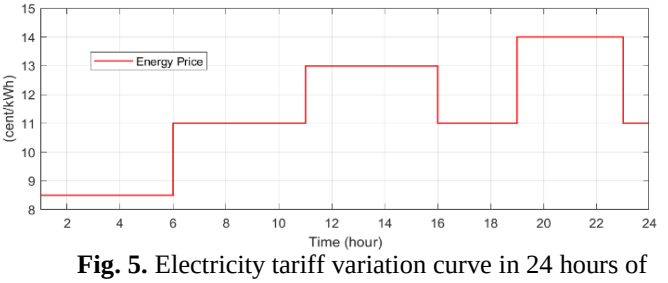

Fig. 5. Electricity tariff variation curve in 24 hours of programming.

The optimization results, including the expected MGO profit, the cost of paying customers, the cost of producing distributed generation units, the emission of greenhouse gases, and the cost of EENS for various tests, are shown in Table 3. This table shows the economic, environmental, and reliability results of the proposed model. According to the results of this table in the first test, despite the high payment of customers, the amount of operating profit is also at its lowest value. In other words, in this test, MGO has to use expensive units to supply the load, especially during peak-load hours.

In the second test, with the participation of responsive loads and reduction of the network peak, the amount of customer's payments for the consumed load has decreased. In this test, the total customers earned 2728.3 cents from participating in DR programs. Therefore, the net payment of customers has been reduced to 119872.05 cents. In other words, the net payment of customers has decreased by 9.25% compared to the first test. Despite MGO's declining revenue from customers and pay for loads participation in the DR program, the operator's expected profit has reached 40,521.4 cents. It has raised to 52.22% compared with the first test. In addition to the economic debate, the value of lost load has significantly decreased and the reliability of the power supply has also increased. Greenhouse gas emissions have also been reduced by more than 340 kg/Day.

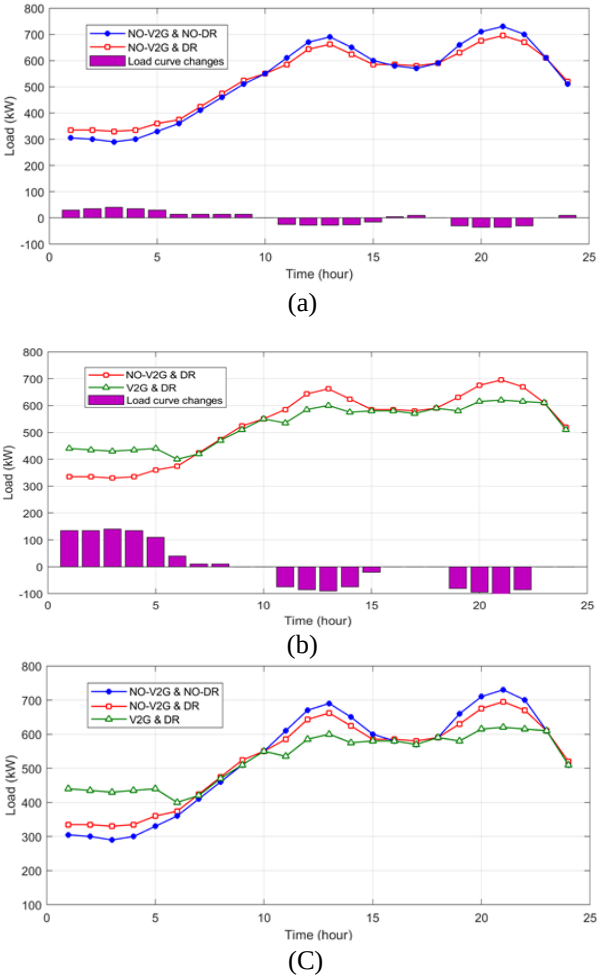

Fig. 6. Load curve variations in different tests: a) Average load curve variations with DR participation. b) Average load curve variations with DR and V2G participation. c) Average load curve variations in three tests.

But in the third test, with the simultaneous participation of responsive loads and electrical feed, the peak load value decreased significantly, resulting in a reduction in customer's payments for electricity to 118,120.1 cents. With the participation of responsive

loads and V2G capability of electric vehicles, the customers have earned a total of 2006.8 and 5100 cents. Therefore, the net payment of customers has been reduced to 111013.3 cents.

In other words, the net payment of customers has decreased by 17.9% compared to the first test. Despite MGO's declining revenue from customers and the high cost of participating in DR and V2G electric vehicles, the operator's expected profit has reached 50,712.1 cents, up 90.5% from the first test, almost doubling. In addition to the economic issue, the amount of load lost has been greatly reduced to almost zero, and the reliability of the power supply has been greatly increased. Greenhouse gas emissions have also been reduced by more than 1,380 kg/Day.

Table 3. Numerical results of various tests.

Title	First test	Second test	Third test
Payment of customers for electricity consumption $(^{cent}/_{Day})$	130872.05	122523	118120.1
The income of customers to participate in the DR program $(^{cent}/_{Day})$	0	2728.3	2006.8
The income of subscribers for V2G vehicle participation $(^{cent}/_{Day})$	0	0	5100
The production cost of units $(^{cent}/_{Day})$	88524	77252	60220
Cost of lost load ($^{cent}/_{Day}$)	15728.2	2021.3	81.20
Greenhouse gas emissions $(^{kg}/_{Day})$	6528.3	6242.3	5200.2
Net customers Payment $(^{cent}/_{Day})$	130872.05	119794.7	111013.3
MGO's expected profit $(^{cent}/_{Day})$	26619.85	40521.4	50712.1

As can be seen from the results of this table, with the participation of customers in demand response and EVs charge and discharge control, on the one hand, customers pay and on the other hand, MGO's profit has increased. This increase is because of the decrease in load during heavy load hours due to participation in demand response programs and optimal charge and discharge of EVs and as a result of not using expensive units. In the following, the superiority of the proposed model in terms of security and technology is shown. Changes in network frequency at different times and scenarios and for three tests are shown in Fig 7.

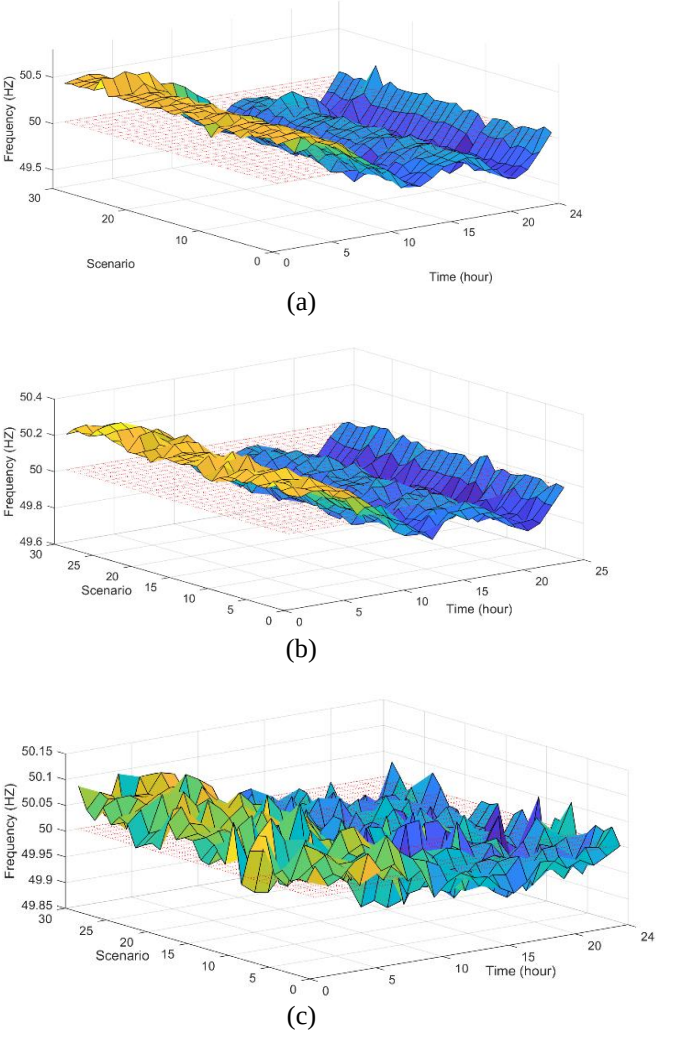

Fig. 7. Micro-grid frequency variations in different scenarios a) test 1 b) test 2 c) test 3.

As shown in Fig 7, in the first test, the frequency variations are very large and close to the allowable range (49.5-50.5). Even in some of the specific scenarios mentioned below, the system frequency is out of range. Using the DR tool, the frequency variations have been reduced and it is in the range of 50.2 to 49.8. However, variations in the micro-grid frequency are still high from low load to peak load hours. In the third test, using the

same DR and V2G strategies, the system frequency is very close to the nominal value and is limited to the range of 49.95 to 50.1. The highest frequency drop (worst case scenario) occurred in Scenario 10. In this scenario, the level of demand and the amount of RESs produced have the highest and lowest values, respectively.

On the other hand, the highest jump for the system frequency occurred in Scenario 25. In this scenario, the demand is the lowest and the production of RESs is the highest. According to these figures, with the participation of final consumers and electric vehicles in the micro-grid operation management program, the system frequency has fewer variations.

The average values of frequency variations in the tests and at different hours are shown in Fig 8. According to this figure, without DR and V2G management, the system frequency is allowed on the eve of leaving the range and the stability margin is very limited.

With the participation of final consumers and electric vehicles during the low load period, despite the increase in load due to peak hours and EVs charging, the average frequency has approached the nominal value. In the third test, with the charge management of electric vehicles along with the responsive loads in the micro-grid utilization management program, the system frequency is very close to the nominal value and its fluctuations are greatly reduced at all hours.

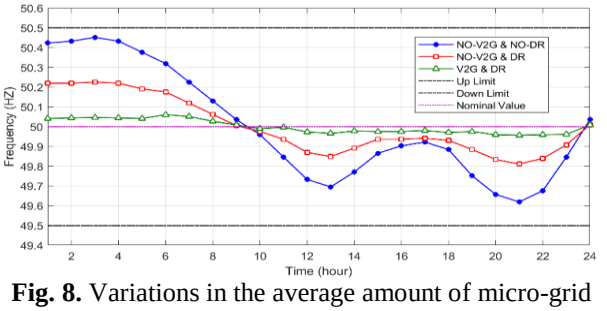

Fig. 8. Variations in the average amount of micro-grid frequency at different hours.

As can be seen from these results, according to the frequency security target in the proposed model, the micro-grid frequency value for all scenarios is set within the allowable range of the nominal frequency. This important goal has been achieved by managing distributed production, DR resources, EVs charge, and discharge control, and by reconciling economic and technical goals.

To observe the significant effect of the proposed strategy, the rate of micro-grid frequency mutation relative to the nominal value is stated in Table 4 and the statistical analysis of frequency variations is provided in Table 5. It should be noted that the allowable deviation of the micro-grid frequency is $\pm 1\%$, i.e., ± 0.5 HZ.

Table 4. Maximum up and down frequencies in different tests.

Title	Maximum up frequency (Hz) Low load) (hours	Maximum down frequency (Hz) (full load hours)	Frequency variations (HZ) From low) to full load (hours
First test	50.45	49.62	0.83
Second test	50.23	49.81	0.42
Third test	50.06	49.96	0.1

Table 5. Standard deviation and variance of frequency in different tests.

Title	Frequency standard deviation(Hz)	Frequency variance	Total frequency error deviations at different hours(Hz)
First test	0.2806	0.0787	5.7267
Second test	0.142	0.0202	2.91
Third test	0.035	0.0013	0.7551

Scenarios 25 and 10, in which the frequency deviations are the highest and lowest values (worst case scenario), are considered as candidates. The results of the frequency deviation for these two scenarios are given in Table 6 to Table 9. The frequency variations of the system for two candidate scenarios and 24 hours of programming are shown in Fig 9 and Fig 10.

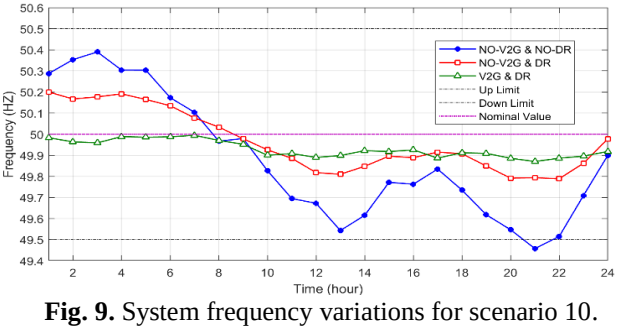

Fig. 9. System frequency variations for scenario 10.

Table 6. Maximum up and down frequency in different tests for Scenario 10.

Title	Maximum up frequency (Hz) Low load) (hours	Maximum down frequency (Hz) (full load hours)	Frequency variations (HZ) From low) to full load (hours
First test	50.3898	49.4579	0.932
Second test	50.199	49.7891	0.4108
Third test	49.995	49.88	0.115

Table 7. Standard deviation and variance of frequency in various tests for Scenario 10.

Title	Frequency standard deviation(Hz)	Frequency variance	Total frequency error deviations at different hours(Hz)
First test	0.2944	0.0867	6.7617
Second test	0.1438	0.0207	3.2076
Third test	0.0398	0.0016	1.06

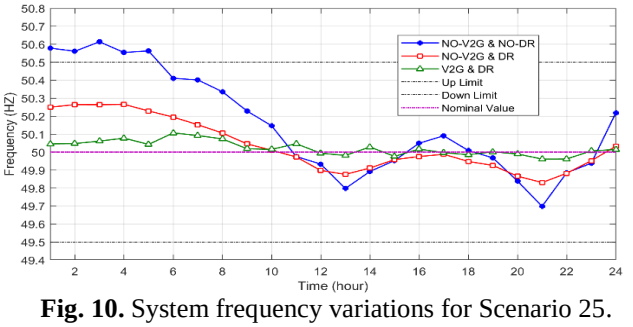

Fig. 10. System frequency variations for Scenario 25.

Table 8. Maximum up and down frequency in different tests for Scenario 25.

Title	Maximum up frequency (Hz) Low load) (hours	Maximum down frequency (Hz) (full load hours)	Frequency variations (HZ) From low) to full load (hours
First test	50.614	49.698	0.9151
Second test	50.266	49.831	0.4351
Third test	50.106	49.962	0.1453

Table 9. Standard deviation and variance of frequency in various tests for Scenario 25.

Title	Frequency standard deviation(Hz)	Frequency variance	Total frequency error deviations at different hours(Hz)
First test	0.2848	0.0811	5.8798
Second test	0.1446	0.0209	2.8281
Third test	0.0402	0.0016	0.8487

According to these figures and tables, in these two special scenarios, the frequency remains in the allowable range for the second and third frequency tests. In other words, in the worst-case scenario, the proposed strategy has been able to maintain frequency security. With simultaneous and correct DR management and charging and discharging of electric vehicles, the frequency adjustment is much more accurate. This difference is quite evident in the results of the second and third tests. The frequency in the first test is out of range. With the proposed strategy in the third test for responsive loads and electric vehicles, the load is transferred from peak hours to non-peak hours, especially low load hours and in addition to a significant reduction in the cost of operating and producing environmental pollutants, the rate of frequency variations has also been greatly reduced and very close to the nominal value. These results show the very acceptable safety and stability margins of the system frequency, which is quite clear from the results of the tables.

In addition to being used in normal situations, in a critical situation, the proposed method can ensure the security of voltage and frequency by compromising economic and security goals. In other words, the proposed method at the time of the disturbance also provides voltage and frequency security. This disturbance can be a sudden exit of one of the units or a sudden change in the production or consumption capacity of the micro-grid. To evaluate the proposed method in critical conditions, according to the N-1 criterion, the DG1 production unit is taken out of the circuit and the frequency response of the system in these conditions is examined for different tests. The results of the frequency response for both scenarios 10 and 25 are shown in Fig 11 and Fig 12.

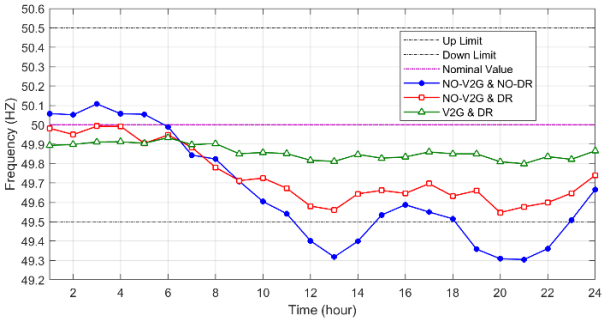

Fig. 11. System frequency variations for scenario 10 in critical situations.

Table 10. Maximum up and down frequency in different tests for Scenario 10 in critical situations.

Title	Maximum up frequency (Hz) Low load) (hours	Maximum down frequency full) (Hz) (load hours	Frequency variations (HZ) From low) to full load (hours
First test	50.11	49.3	0.81
Second test	49.99	49.55	0.44
Third test	49.94	49.8	0.14

Table 11. Standard deviation and variance of frequency in various tests for Scenario 10 in critical situations.

Title	Frequency standard deviation(Hz)	Frequency variance	Total frequency error deviations at different hours(Hz)
First test	0.2775	0.077	9.01
Second test	0.1497	0.0224	6.27
Third test	0.0383	0.0015	2.33

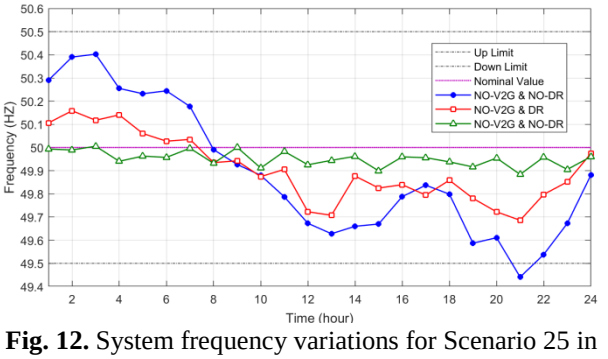

Fig. 12. System frequency variations for Scenario 25 in critical situations.

Table 12. Maximum up and down frequency in different tests for Scenario 25 in critical situations.

Title	Maximum up frequency (Hz) Low load) (hours	Maximum down frequency full) (Hz) (load hours	Frequency variations (HZ) From low) to full load (hours
First test	50.4	49.44	0.96
Second test	50.16	49.69	0.47
Third test	50.01	49.88	0.13

Table 13 Standard deviation and variance of frequency in various tests for Scenario 25 in critical situations.

title	Frequency standard deviation(Hz)	Frequency variance	Total frequency error deviations at different hours(Hz)
First test	0.2892	0.0836	5.8798
Second test	0.1443	0.0208	2.8281
Third test	0.0336	0.0011	0.8487

Since scenarios 10 and 25 are the worst possible scenario in the normal condition, with the occurrence disturbance, the possibility of micro-grid instability is very likely, especially in scenario 10. According to the above results, with the outage of DG1 and the decrease in micro-grid production capacity, the frequency response of the system, especially in scenario 10, which has the highest peak load and the lowest amount of renewable resources production, has become very critical so that, in full load period, the system frequency is out of the allowable range and the frequency security is disrupted. Since in tests 2 and 3, the system frequency security was in good condition and the micro-grid stability margin was high, with the outage of the DG1, the frequency is still within the allowable range. According to the results, especially in the third test with V2G and G2V management, along with DR management, the margin of safety and stability of the system frequency is still in the desired value.

The level of reactive power in the buses determines the amount of voltage. In buses with DG, If the reactive power injection rate decreases, the voltage magnitude will also be reduced. In load buses, If the amount of demand changes, the amount of reactive power will change, and the voltage at that bus will change.

However, it should be noted that the reactive power injected or absorbed by a production unit or a consumption load can also affect the voltage of adjacent buses. The proposed strategy is designed in such a way that in addition to frequency security, it also ensures network voltage security. In other words, by compromising between different goals, the reactive power of distributed generations is adjusted so that the bus voltage has the lowest drop. Similar to frequency security, the operator is also able to improve bus voltage by using two tools for managing responsive loads and managing to charge and discharging electric vehicles.

Fig 13 shows the load distribution at different buses. At a time of day when the load is at its peak, the voltage of the buses has the highest drop. For this reason, the peak hour, which is 21 o'clock according to Fig 6, has been selected as the sample hour to check the bus voltage.

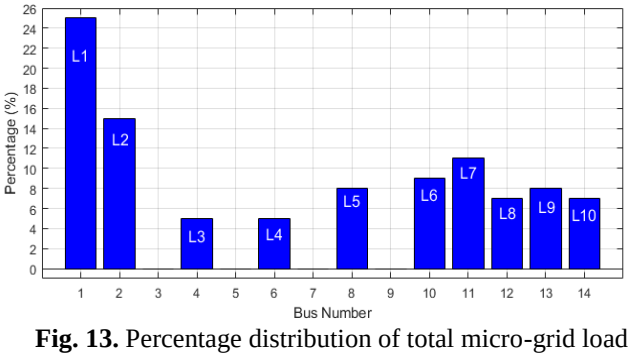

Fig. 13. Percentage distribution of total micro-grid load per hour at different buses.

As explained earlier, in Scenario 10, the amount of renewable resource production is the lowest and the load is the highest possible. Fig 14 shows the voltage variations of the micro-grid buses in Scenario 10 and at 9 pm, the network peak hour. In this case, the micro-grid has the highest voltage drop.

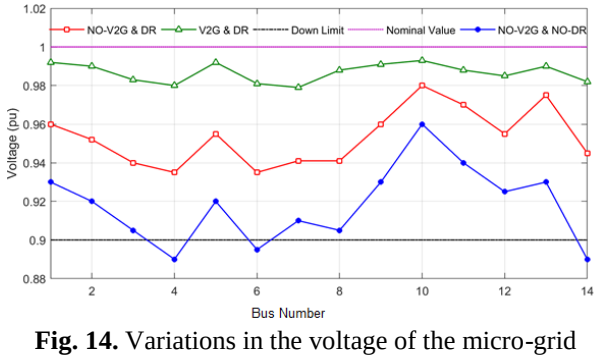

Fig. 14. Variations in the voltage of the micro-grid buses in scenario 10 and at 21:00 (normal conditions).

As shown in Fig 14, without managing responsive loads and electric vehicles in the first test, the bus voltage drop is high. This voltage drop is especially high at the end buses of branches and buses that do not have scattered products so that in 3 buses of the network, the voltage exceeds the allowable value. It should be noted that the allowable amount of voltage drop in the micro-grid is $\pm 10\%$ and the base voltage value of 380V is considered. Therefore, the allowable value of the voltage drop is $\pm$ 0.1pu.

Applying responsive loads leads to improving the grid voltage and the voltage of all buses are within the allowable range. In the third test, with the charge management of electric vehicles, in addition to reducing the charge in peak hours, a large part of the load is also provided by V2G electric vehicles. Therefore, as it is known, with the simultaneous management of responsive loads and charging and discharging of electric vehicles, the amount of voltage drop has been greatly reduced and the voltage stability margin has been greatly increased.

Similar to the previous section, in critical situations, and the occurrence of disturbances, the voltage status of micro-grid buses has been investigated. As the DG1 outage, the voltage drop of bus 1 increases. As the voltage drop of bus 1 increases, the other connected buses also increase their voltage drop. The voltage results of the buses in critical conditions and the outage of the DG1 unit for scenario 10 and at 21:00 are shown in Fig 15. According to this figure, in the first test, the micro-grid voltage is unstable and in many cases, the value of the voltage range exceeds the allowable value. Therefore, without the proposed strategy, the continuation of the micro-grid will be disrupted. By applying responsive loads in the second test, the voltage drop is reduced but the voltage safety margin is still low. In the third test, with the simultaneous use and management of responsive loads and V2G mode of electric vehicles, in addition to reducing the voltage drop, the voltage safety is also maintained to the desired level. Fig 14 and Fig 15 illustrate the optimal performance of the proposed strategy in maintaining network voltage safety under normal and critical conditions.

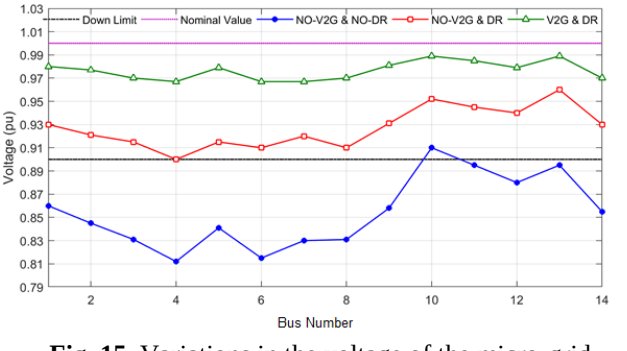

Fig. 15. Variations in the voltage of the micro-grid buses in scenario 10 and at 21:00 (critical conditions).

4. CONCLUSION

4.1. Summery

This paper addresses the issue of optimizing multi-objective economic and security goals for micro-grids based on distributed generations, along with charge and discharge management of electric vehicles and responsive loads. To smooth the daily load curve, the shift of energy consumption from peak hours to other hours has been used with responsive load management tools and the strategy of controlling the charge and discharge of electric vehicles. With the simultaneous participation of responsive loads and electric vehicles, the load curve is modified and leveled. With the simultaneous participation of responsible loads and electric vehicles, the load curve is modified and flatted. Net customer payments decreased by 17.9%. Despite MGO's declining revenue from customers and paying for the participation of loads in the DR program and electric vehicles in the V2G program, the expected profit of the operator has increased by 90.5% and has almost doubled. In addition to the economic debate, the value of lost load has been greatly reduced to almost zero, and the reliability of the power supply has been greatly increased. Greenhouse gas emissions have also been reduced by more than 1,380 kg/Day. According to the results of voltage and frequency security, both were analyzed in the worst-case scenario for both normal and critical states. The proposed strategy has well-maintained voltage and frequency security and maintained a stable margin in the desired value. In summary, this paper introduces a management strategy for managing the penetration of electric vehicles along with responsive loads. The strategy pursued several goals, including reducing energy and load costs, reducing the cost of charging EVs, and improving network parameters and security, such as voltage and frequency. Based on the results, the proposed approach has been able to turn the challenge of electric vehicle penetration into an opportunity to improve network parameters and even reduce energy costs. By managing the EVs charge at low load and intermediate load and using the remaining energy in the EVs battery during heavy hours, along with the demand management program, the cost of energy supply is greatly reduced and the load characteristic is flattened. On the other hand, the decrease in network peak and load distribution at different hours along with the management of responsive loads, has improved voltage and frequency security, especially in the end buses of each branch. The results confirm the effectiveness of the proposed approach.

4.2. Future work

Some challenges and future research are discussed below.

- **Allocating of distributed generations and charging stations for electric vehicles in the network:** The high penetration of electric vehicles and their performance, whether in the form of V2G or G2V, along with distributed generation, requires changes in the distribution network. The location of smart parking lots and charging stations and the installation of distributed generation with economic and stability goals, with the least change in the network, are the research topics of recent years.

- **New control strategies to improve micro-grid stability:** IIDGs usually have high response speeds and low inertia; therefore, the stability of these types of DGs is easily affected by disturbance. Introducing a new control strategy to increase micro-grid stability with proper charge and discharge management of electric vehicles is one of the research topics in the coming years.

- **Optimal micro-grid design methods:** All topics covered during this study are categorized in the field of operation studies. In the field of planning, the research gap is quite felt. Micro-grid stability analysis can be used for optimal and reliable micro-grid design. For example, energy storage DGs are very effective in maintaining micro-grid stability, but the capacity of these resources is debatable. Location of DGs, location of smart parking lots, optimal capacity of micro-grid equipment, etc. is also among the topics in this area.

- **Optimal operation of energy hub with the management of economic and environmental loads:** Gas carriers along with electricity carriers have developed a lot in recent years. Since most of the load consumption of micro-grids is thermal load and considering the development of CHP products, providing a probabilistic model for energy management in the short term to achieve the minimum operating cost in a micro-grid modeled as an energy hub along with environmental issues can be one of the objectives of the research in the future. Due to the random behavior of wind and solar energy, accurate prediction of the potential of distributed generation based on renewable energy is not possible and is

always associated with uncertainty errors in the planning of the next day.

- **High penetration of micro-grids and renewable resources in the power network structure:** The increasing growth of renewable resources and consequently the high penetration of micro-grids in the power grid structure in the coming years are undeniable. The behavior of the power grid with the high penetration of micro-grids could be one of the future researches.

Practical evaluation of the results of this research is currently not possible in Iran. Since the electricity networks in the distribution and purchase of electricity are not private in the first place and secondly, the distribution networks are not smart and these two conditions must be met for the practical implementation of the project.

ABBREVIATIONS

MG	Micro-grid
MGO	Micro-grid operator
DR	Demand response
DG	Distributed generation
RES	Renewable energy source
BEV	Battery electric vehicle
WT	Wind turbine
PV	Photo-voltaic (solar-power)
PHEV	Plug-in hybrid electric vehicle
SOC	State of charge
G2V	Grid-to-vehicle
V2G	Vehicle-to-grid

REFERENCES

[1] N. Rezaei, M. J. I. J. o. E. P. Kalantar, and E. Systems, **"Stochastic frequency-security constrained energy and reserve management of an inverter interfaced islanded microgrid considering demand response programs"**. *International journal of electrical power & energy*. Vol.69. pp. 273-286. 2015.

[2] P. P .Vergara, J. C. López, J. M. Rey, L. C. da Silva, and M. J. Rider, **"Energy management in microgrids. Microgrids design and implementation"**. Springer. pp.195-216. 2019.

[3] Y. Noorollahi, A. Aligholian, A. J. J. o. E. M. Golshanfard, **"Stochastic energy modeling with consideration of electrical vehicles and renewable energy resources-A review"**. *Journal of energy management and technology*. Vol. 4. No. 1. pp. 13-26. 2020.

[4] H. Kaur and I. Kaur, **"Optimization and control of hybrid renewable energy systems: A review"**. *in Cognitive informatics and soft computing*. pp. 483-500. 2020.

[5] A. Singh and S. J. S. S. Suhag, **"Trends in islanded microgrid frequency regulation–a review"**. *Smart science*. Vol. 7. No. 2. pp. 91-115. 2019.

[6] M. Ghahramani, M. Nazari-Heris, K. Zare, and B. Mohammadi-ivatloo, **"Robust short-term Scheduling of smart distribution systems considering renewable sources and demand response programs"**. *in robust optimal planning and operation of electrical energy systems: Springer*. pp. 253-270. 2019.

[7] M. Mazidi, H. Monsef, and P. J. A. e. Siano, **"Robust day-ahead scheduling of smart distribution networks considering demand response programs"**. *Applied energy*. Vol. 178. pp. 929-942. 2016.

[8] N. Rezaei, M. J. E. c. Kalantar, **"Economic–environmental hierarchical frequency management of a droop-controlled islanded microgrid"**. E*nergy conversion and management*. Vol. 88. pp. 498-515, 2014.

[9] S. Conti, R. Nicolosi, S. Rizzo, and H. J. I. T. o. P. D. Zeineldin, **"Optimal dispatching of distributed generators and storage systems for MV islanded microgrids"**. *IEEE transactions on power delivery*. Vol. 27 ,No. 3. pp. 1243-1251. 2012.

[`10] J.-M. Clairand, M. Arriaga, C. A. Canizares, and C. J. I. T. o. S. E. Alvarez, **"Power generation planning of galapagos Microgrid considering electric vehicles and induction stoves"**. *IEEE transactions on sustainable energy*. Vol. 10 ,No. 4. pp. 1916-1926.2018.

[11] S. H. Shamsdin, A. Seifi, M .Rostami-Shahrbabaki, and B. Rahrovi, **"Plug-in electric vehicle optimization and management charging in a smart parking lot"**, in 2019 IEEE Texas power and energy conference (TPEC). pp. 1-7: IEEE. 2019.

[12] G. Heppeler, M. Sonntag, U. Wohlhaupter, and O .J. C. E. P. **"Sawodny,Predictive planning of optimal velocity and state of charge trajectories for hybrid electric vehicles"**. *Control engineering practice*. vol. 61. pp. 229-243. 2017.

[13] Z. Darabi, P. Fajri, and M. J. I. T. o. I. T. S. Ferdowsi, **"Intelligent charge rate optimization of PHEVs incorporating driver satisfaction and grid constraints"**. *IEEE transactions on intelligent transportation systems*. Vol. 18. No. 5. pp. 1325-1332. 2017.

[14] M. R. Sarker, Y. Dvorkin, and M. A. J. I. T. o. P. S. Ortega-Vazquez, **"Optimal participation of an electric vehicle aggregator in day-ahead energy and reserve markets"**. *IEEE transactions on power systems*. Vol. 31. No. 5. pp. 3506-3515. 2016.

[15] M. Pourbehzadi *et al.* **"Optimal operation of hybrid AC/DC microgrids under uncertainty of renewable energy resources: A comprehensive review"**. *International journal of electrical power & energy systems*. Vol. 109. pp. 139-159. 2019.

[16] T. Hoogvliet, G. Litjens, and W. Van Sark , **"Provision of regulating-and reserve power by electric vehicle owners in the Dutch market"**. *Applied energy*. Vol. 190. pp. 1008-1019. 2017.

[17] P. Firouzmakan, R.-A. Hooshmand, M. Bornapour, A. J. R. Khodabakhshian, and S. E .Reviews, **"A comprehensive stochastic energy management system of micro-CHP units, renewable energy**

sources and storage systems in microgrids considering demand response programs". *Renewable and sustainable energy reviews*. Vol. 108. pp. 355-368. 2019.

[18] D. K. Dheer, N. Soni, S. J. S. E. Doolla , Grids, and Networks, **"Improvement of small signal stability margin and transient response in inverter-dominated microgrids. Sustainable energy"**, *grids and networks*. Vol. 5. pp. 135-147. 2016.

[19] A. A. Moghaddam, A. Seifi, T. Niknam, and M. R. A. J. E. Pahlavani, **"Multi-objective operation management of a renewable MG (micro-grid) with back-up micro-turbine/fuel cell/battery hybrid power source"**. *energy*. Vol. 36. No. 11. pp. 6490-6507. 2011.

[20] S. Shafiee, M. Fotuhi-Firuzabad, and M. J. I. T. o. S. G. Rastegar, **"Investigating the impacts of plug-in hybrid electric vehicles on power distribution systems"**. *IEEE transactions on smart grid*. Vol. 4. No. 3. pp. 1351-1360. 2013.

[21] M. Vahedipour-Dahraie, H. R. Najafi, A. Anvari-Moghaddam, and J. M. J. A. S. Guerrero. **"Study of the effect of time-based rate demand response programs on stochastic day-ahead energy and reserve scheduling in islanded residential microgrids"**. *Applied Sciences*. Vol. 7. No. 4. p. 378. 2017.

[22] M Ou, Y Xue, XP Zhang,**" Iterative DC optimal power flow considering transmission network loss"**. *Electric Power Components and Systems, Taylor & Francis*. 2016.

[23] T Akbari, MT Bina,**" Linear approximated formulation of AC optimal power flow using binary discretisation"**. *IET Generation, Transmission & Distribution*, 2016.

[24] Bakhshinejad, A., Tavakoli, A. & Moghaddam, M.M. **"Modeling and simultaneous management of electric vehicle penetration and demand response to improve distribution network performance"**. *Electric Engineering*, 2020.